Invited talk. To appear on: Issues in unifications of AGNs
ASP Conference Series, Vol. ???, 2002
eds. R. Maiolino, A. Marconi & N. Nagar

The evolution of AGNs in the Hard X-Rays and the Infrared

Fabio La Franca, Israel Matute

Dipartimento di Fisica, Università degli studi "Roma Tre", Via della Vasca Navale 84, I-00146 Roma, Italy

Fabrizio Fiore

Osservatorio Astronomico di Roma, Via Frascati 33, I-00040 Monteporzio, Italy

Carlotta Gruppioni, Francesca Pozzi, Cristian Vignali

Osservatorio Astronomico di Bologna, Via Ranzani 1, I-40127 Bologna, Italy

on behalf of the HELLAS and ELAIS consortii[1]

Abstract. We present the estimate of the evolution of type 1 AGNs in the hard (2-10 keV) X-rays drawn from the HELLAS survey, and in the IR (15 μm) obtained from the ELAIS survey. We find that the local luminosity function (LF) of AGN1 in the 2-10 keV is fairly well represented by a double-power-law-function. There is evidence for significant cosmological evolution according to a pure luminosity evolution model $L_X(z)\propto(1+z)^k$, with k=$2.12^{+0.13}_{-0.14}$ and k=$2.19^{+0.13}_{-0.14}$ in a (Ω_m,Ω_λ)=(1.0,0.0) and in a (Ω_m,Ω_λ)=(0.3,0.7) cosmology respectively. In a (Ω_m,Ω_λ)=(1.0,0.0) Universe the data show an excess of faint high redshift type 1 AGN which is well modeled by a luminosity dependent density evolution, similarly to what observed in the soft X-rays. In the IR band, with a (Ω_m,Ω_λ)=(1.0,0.0) cosmology, similarly to what observed in other wavebands, the LF is a double-power-law-function with a bright slope 2.7 and a faint slope 1.0, following a luminosity evolution model $L_{IR}(z)\propto(1+z)^{3.3}$.

1. Introduction

Before the advent of the last generation of hard X-ray telescopes, AGN samples were predominantly based on type 1 objects (AGN1[2]) selected either in the optical or later on in the soft X-rays by ROSAT. In these bands the evolution

[1]HELLAS: A. Antonelli, A. Comastri, P. Giommi, G. Matt, S. Molendi, G.C. Perola, F. Pompilio. ELAIS: C. Lari, M. Mignoli, G. Zamorani, D. Alexander, S. Oliver, S. Serjeant, A. Franceschini, G. Danese, M. Rowan-Robinson.

[2]We here define AGN1 all the AGNs having a broad emission line spectrum in the optical.

of AGN1 has been well measured (see e.g. Della Ceca et al. 1992; Boyle et al. 2000; Miyaji, Hasinger and Schmidt 2000). On the contrary the generation of samples of type 2 AGNs (AGN2) has been difficult at any wavelength and limited to few local surveys.

The general picture was in favor of a model in which type 1 objects were associated to AGNs with low absorption in the X-rays while type 2 to obscured sources with large column densities and spectra strongly depressed in the soft X-rays and emitting mainly in the a) hard X-rays and b) mid and far infrared. For these reasons, in order to achieve a more exhaustive picture of the evolution of the whole family of AGNs, the researches have been recently concentrated in these two wavebands.

Thanks to their high angular resolution ($\sim$1-5 $''$) the first spectroscopic identification projects of faint *Chandra* and *XMM-Newton* hard X-ray sources have been able to observe faint (I$\sim$23) optical counterparts. At variance with the classical type-1/type-2 model in the optical, a significant number of the counterparts ($\sim$30%) resulted to be apparently optical normal galaxies, and moreover part of the optical type 1 AGNs resulted to be absorbed in the hard X-rays (see e.g. Fiore et al. 2000; Comastri et al. 2001; Barger et al. 2001).

These observations have complicated the picture of the AGN model. In the framework of the computation of the density of AGNs, it is not clear how to handle the classification of the sources and to take into account the selection biases introduced by the observation in the 2-10 keV range where the absorption still play a relevant role.

At variance, the situation in the mid infrared is in a less advanced stage because of the scarcity of satellite missions, the only ones being *IRAS* and *ISO*. Although the *ISO* mission has been completed a couple of years ago, the only existing survey of AGN in the mid infrared is still the sample from Rush, Malkan and Spinoglio (RMS, 1993) obtained from the IRAS observations of the whole sky at 12 μm down to $\sim$300 mJy. We have thus decided to undertake two projects.

a) While the recent deep surveys with *Chandra* and *XMM-Newton* have reached fluxes $\sim 2 \times 10^{-16} erg\ cm^{-2} s^{-1}$ (2-8 keV, Brandt et al. 2001) in quite small areas (less than 1 deg^2), at brighter fluxes ($\sim 10^{-13} erg\ cm^{-2} s^{-1}$; 5-10 keV) the density of sources is low (about 5/deg^2) and tenths of square degrees are to be covered in order to collect statistical significant samples. Such samples are quite rare at moment but are essential in order to fully cover the X-ray luminosity/redshift plane and study the AGN evolution. In the first part of this paper we report the results of the spectroscopic identifications of one of such samples (HELLAS), which covers from 0.2 to 55 deg^2 in the flux range $5 \times 10^{-14} - 5 \times 10^{-11} erg\ cm^{-2} s^{-1}$ (5-10 keV).

b) In order to extend at deeper fluxes the coverage of the luminosity redshift plane in the mid infrared (15 μm) we have carried out the European Large Area ISO Survey (ELAIS) over 12 deg^2 down to $\sim$0.5-1 mJy, more than 2 order of magnitudes deeper than the previous RMS sample. In the second part of this paper we will report on the results of the spectroscopic identifications of this project.

2. HELLAS: The evolution of AGN1 in the Hard X-ray

2.1. The HELLAS survey

The X-ray sources have been detected by the *BeppoSAX*-MECS instruments in the 5-10 keV band in the framework of the High Energy Large Area Survey (HELLAS). Preliminary results have been presented in Fiore et al. (1999). The whole survey and the catalogue used in this study is described by Fiore et al. (2001). The data have been analyzed in the framework of the synthesis models for the X-ray background by Comastri et al. (2001), and the correlation with the soft X-rays has been investigated by Vignali et al. (2001).

The spectroscopic follow up of the HELLAS sources has been carried out in a subsample of 118 sources out of a total of 147. The *BeppoSAX* X-ray positions have an uncertainty of about 1-1.5 arcmin depending on the distance of the sources from the axis of the telescope. We have thus searched for optical counterparts having R magnitude brighter than 20.5-21.0 in a circular region of 1-1.5 arcmin of radius around the HELLAS positions. In the case of large off-axis distances, the larger error-boxes ($1.5''$) have been used. 25 sources have been identified with cross-correlation with existing catalogues available from NED, and 49 have been investigated at the telescope.

We have divided the identified sources in AGN1, AGN2, galaxies with narrow emission lines showing moderate-to-high degree of excitation (ELG), and stars. AGN2 includes AGN1.5, AGN1.8 and AGN1.9. No distinction has been done among radio-loud and radio quite objects. The R-band magnitudes of these identifications have been pushed down to the limit of obtaining less than 10% probability of having a spurious identification due to chance coincidences for each of the HELLAS sources (i.e. 90% reliability for the whole sample).

For AGN1 we have chosen a limit of R=21 where the surface density is $\sim$60-70/deg^2. We have chosen a limit of R=19 for AGN2. We have collected all the objects which are mainly starburst galaxies and low ionization narrow emission line galaxies (LINERS) within the class of emission line galaxies (ELG). For these objects a limit of R=17.5 has been chosen. In total, 63% (74/118) of our HELLAS subsample has been searched for spectroscopic identification. 61 have been identified: 37 AGN1, 9 AGN2, 5 ELG, 6 Clusters, 2 BL Lac, 1 Radio Galaxy and 1 Star.

2.2. The evolution of AGN1

For the reasons described before we have decided, at moment, to limit the analysis of the evolution of AGN to the AGN1 only. We have assumed H_0=50 km/s/Mpc and either the (Ω_m,Ω_Λ)=(1.0,0.0) or the (Ω_m,Ω_Λ)=(0.3,0.7) cosmologies. In order to join our data with other existing samples we have computed the 2-10 keV luminosity for type 1 AGN assuming a typical spectral energy distribution as computed by Pompilio, La Franca & Matt (2000), which is roughly approximated by a single power slope in energy with index 0.6 ($\frac{dF}{dE} \propto E^{-0.6}$) in the range 2-50 keV (i.e. up to z=4).

The statistical significance of our analysis has been increased by joining our data to other hard X-ray samples of AGN1 identified by Grossan (1992), Boyle et al. (1998), and Akiyama et al. (2000).

We carried out a least-squares method to derive best-fit parameters for the 2-10 keV luminosity function (LF) and its cosmological evolution. All the fits have been tested with the bidimensional Kolmogorov-Smirnov test (2DKS). The summary of the results is presented in Table 1. Two different functional forms have been used. Following Boyle et al. (1998) and Ceballos and Barcons (1996), we used the pure luminosity evolution (PLE) for the QSO LF. We also used the luminosity dependent density evolution (LDDE) model similar to the one fitted in the soft X-rays by Miyaji et al. (2000).

The local (z=0) QSO LF used for the PLE model has been represented by a two-power-law:

$$\begin{array}{ll} \frac{d\Phi(L_X)}{dL_X} = A(L_X^{*(\gamma_1-\gamma_2)})L_X^{-\gamma_1} & : L_X \leq L_X^*(z=0), \\ \frac{d\Phi(L_X)}{dL_X} = AL_X^{-\gamma_2} & : L_X > L_X^*(z=0), \end{array}$$

where L_X is expressed in units of $10^{44}\mathrm{erg\,s^{-1}}$. A standard power-law luminosity evolution model was used to parameterize the cosmological evolution of this LF: $L_X^*(z) = L_X^*(0)(1+z)^k$.

In the case of the LDDE model, as an analytical expression of the present day ($z = 0$) luminosity function, we used the smoothly connected two power-law form:

$$\frac{d\Phi(L_\mathrm{x}, z=0)}{d\mathrm{Log}L_\mathrm{x}} = A[(L_\mathrm{x}/L_*)^{\gamma_1} + (L_\mathrm{x}/L_*)^{\gamma_2}]^{-1}.$$

The description of the evolution is given by a factor $e(L_\mathrm{x}, z)$ such that:

$$\frac{d\Phi(L_\mathrm{x}, z)}{d\mathrm{Log}L_\mathrm{x}} = \frac{d\Phi(L_\mathrm{x}, z=0)}{d\mathrm{Log}L_\mathrm{x}} \times e(L_\mathrm{x}, z),$$

where

$$e(L_\mathrm{x}, z) = \begin{cases} (1+z)^{\max(0, p1-\alpha\,\mathrm{Log}\,[L_\mathrm{a}/L_\mathrm{x}])} & (z \leq z_\mathrm{c}; L_\mathrm{x} < L_\mathrm{a}) \\ (1+z)^{p1} & (z \leq z_\mathrm{c}; L_\mathrm{x} \geq L_\mathrm{a}) \\ e(L_\mathrm{x}, z_\mathrm{c})\,[(1+z)/(1+z_\mathrm{c})]^{p2} & (z > z_\mathrm{c}). \end{cases}$$

We started our computation of the luminosity function in an (Ω_m,Ω_Λ)=(1.0,0.0) cosmology. The only previous estimate of the evolution of AGN1 in the 2-10 keV range was from Boyle et al. (1998), who joined the local sample of 84 AGN1 observed by *HEAO1* from Grossan (1992) with a fainter sample of 12 AGN1 observed by *ASCA* (see their distribution in the L_X-z plane in Figure 1a).

In Figure 1b the luminosity function from only our 37 AGN1 from HELLAS in three redshift intervals ($0.0 < z < 0.2$, $0.2 < z < 1.0$, and $1.0 < z < 3.0$) is shown. For comparison the best fit luminosity function from Boyle et al. (1998) is also shown. The data have been represented by correcting for evolution within the redshift bins as explained in La Franca and Cristiani (1997). The data are in rough agreement with the previous estimate of Boyle et al. (1998), but show some evidence of an excess of faint AGN1 at redshifts larger than $z \sim$0.3. This

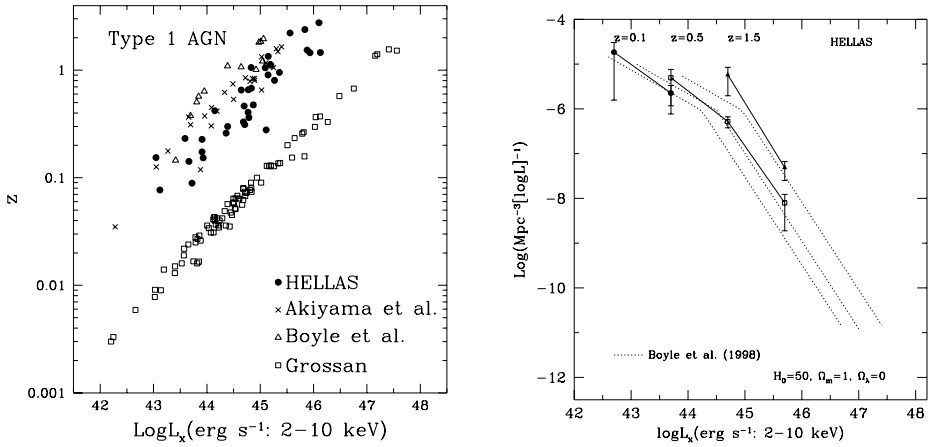

Figure 1. a) The luminosity/redshift distribution for all the 156 AGN1 used to compute the hard X-ray 2-10 keV luminosity function. They include 37 AGN1 from HELLAS, 82 AGN1 from Grossan, 12 AGN1 from Boyle et al. (1998) and 25 AGN1 from Akiyama et al. (2000). b) The luminosity function of the 37 type 1 AGN from HELLAS. The dotted lines show, as a reference, the previously estimated luminosity function in the 2-10 keV from Boyle et al. (1998). The densities have been corrected for evolution within the redshift bins.

feature is strengthened by joining our data with the other AGN1 samples from Grossan (1992), Boyle et al. (1998), and Akiyama et al. (2000) (see Figure 2a). These samples all together collect 156 AGN1. These data have a (χ^2) 0.04 probability to be drawn from a PLE model such as that computed by Boyle et al. (1998, see model 0 in Table 1). Our best fit to the whole data with a PLE model found similar parameters as those of Boyle et al. (1998) but a slightly larger evolution ($k = 2.13$ instead of $k = 2.04$) and a significantly larger normalization (model 1). This difference is originated by the necessity of better fitting the observed higher density of faint AGN1 at high redshifts. The 2DKS test gives a probability of 0.22 for this fit (see Figure 2a and Table 1). A even better probability of 0.31 is obtained if a stop in the evolution is applied at redshift $z_{cut} = 1.39$ and a larger evolution ($k = 2.52$) is used (model 2).

Although our fits are already statistically adequate, our PLE model is not able to fully describe the observed over-density of faint AGN1 at high redshifts. As this feature is quite similar with what observed in the soft X-rays (Miyaji et al. 2000) we tried to get a even better fit by using the luminosity dependent density evolution (LDDE) model similar to the one fitted in the soft X-rays. We first kept fixed all the parameters to the values found in the soft X-rays, just leaving L_* free to vary (model 3). The 2DKS test gives a probability of 0.11. The value LogL_*=44.13 found by our fit nearly corresponds to the value LogL_*=43.78 found in the soft X-rays if a linear relation L_X(0.5-2 keV)=0.471×L$_X$(2-10 keV) is assumed, which corresponds to the slope 0.6 of the AGN1 spectra which we used in this analysis. Later we kept fixed just $z_c = 1.55$ and $\alpha = 2.5$ to the value found by Miyaji et al. (2000) for AGN1 only, and left all the remaining

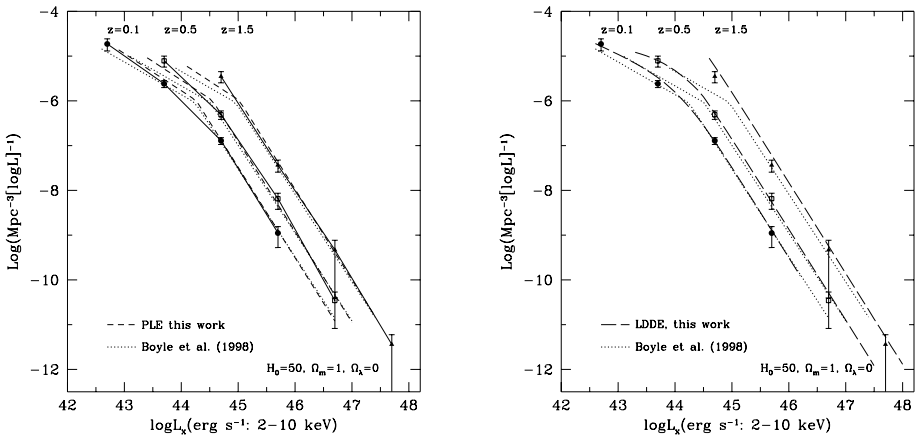

Figure 2. a) The luminosity function of the total sample of 156 AGN1 including the 37 AGN1 from HELLAS, 82 AGN1 from Grossan, 12 AGN1 from Boyle et al. (1998) and 25 AGN1 from Akiyama et al. (2000). The excess of faint AGN1 at high redshifts is even more evident than in the previous figure. The dotted line is the PLE fit (model 0, Table 1) by Boyle et al. (1998). The dashed line is our best PLE fit (model 1, Table 1). b) The luminosity function of AGN1 fitted with the LDDE model (model 4 in Table 1, see text).

parameters free to vary (model 4, see Figure 2b). In this case the 2DKS test gives a probability of 0.47.

Although we find a better fit of the data with the LDDE model, the existing sample is not able to distinguish between PLE and LDDE. In Figure 3a the differential counts of the 156 AGN1 used in the evaluation of the evolution of the LF is shown. The continuous line is the prediction of the LDDE/b model while the dashed line is the prediction of the PLE model with z_{cut}. $(\Omega_m, \Omega_\Lambda)$=(1.0,0.0) is assumed. The two models differentiates at fluxes fainter than $f_{2-10keV} \sim 10^{-13} erg\ cm^{-2} s^{-1}$, where the LDDE/b model predicts a higher density of AGN1. The new upcoming fainter surveys from *Chandra* and *XMM-Newton* will easily test which model is correct.

Our best fit LF LDDE/b model predicts a contribution of AGN1 to the 2-10 keV X-ray background of $I_{2-10} = 1.04 \times 10^{-11}$ erg cm^{-2} s^{-1} deg^{-2}, while the PLE model with z_{cut} predicts $I_{2-10} = 0.76 \times 10^{-11}$ erg cm^{-2} s^{-1} deg^{-2}. These values correspond to a fraction of 53% and 39% respectively of the 2-10 keV X-ray background (we used $I_{2-10} = 1.95 \times 10^{-11}$ erg cm^{-2} s^{-1} deg^{-2} from Chen, Fabian and Gendreau 1997).

If an $(\Omega_m,\Omega_\Lambda)$=(0.3,0.7) cosmology is assumed the PLE models obtain an ever better representation of the data in comparison with what found in the $(\Omega_m,\Omega_\Lambda)$=(1.0,0.0) Universe (see Table 1, models 5 and 6). The 2DKS probability is 0.73 and 0.48, with and without the introduction of the z_{cut} parameter respectively. In this case even the simple PLE model obtains a quite good fit of the data (Figure 3b), and the introduction of the z_{cut} parameter is necessary to stop the evolution only at redshifts larger than 2.3. However our data contain

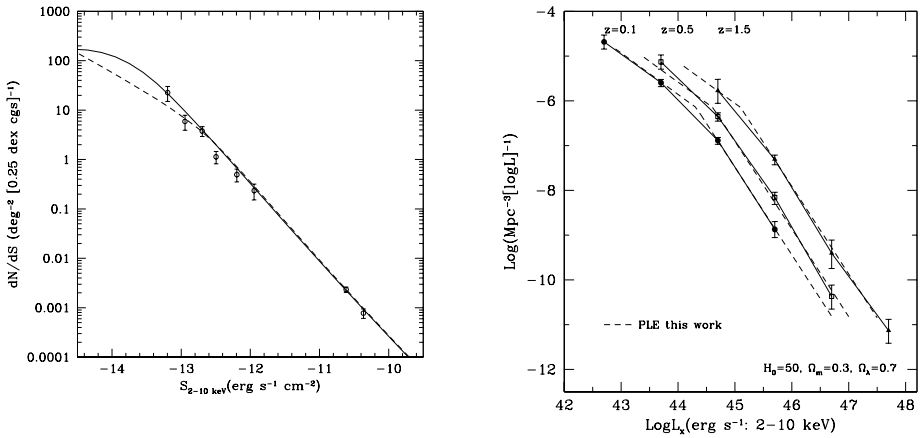

Figure 3. a) The differential counts of AGN1. The continuous line is the expected counts for the LDDE/b model. The dashed line is the expected counts for the PLE model with z_{cut}. $(\Omega_m, \Omega_\Lambda)$=(1.0,0.0) is assumed. b) The luminosity function in the $(\Omega_m, \Omega_\Lambda)$=(0.3,0.7) Universe fitted by our PLE model (model 5 in Table 1).

not enough AGN1 at redshift larger than 2 in order to obtain an accurate measure of the z_{cut} parameter (see Figure 1a), and the errors in this parameter are quite large.

3. ELAIS: The evolution of AGN1 in the MIR (15μm)

3.1. The ELAIS survey

The European Large Area ISO Survey (ELAIS) is the largest single open time project conduced by ISO, mapping an area of 12 deg^2 at 15μm with ISOCAM and at 90μm with ISOPHOT. Four main fields were chosen (N1, N2, N3 in the north hemisphere and S1 in the south) at high Ecliptic latitudes ($|\beta| > 40^o$).

Table 1. The 2-10 keV AGN LF parameters

Model	γ_1	γ_2	LogL^*	k *or* $p1$	z_{cut}	A^a	P_{2DKS}
0) PLE from Boyle*	1.73	2.96	44.16	2.00	...	8.2×10^{-7}	0.04^b
1) PLE*	1.83	3.00	44.17	2.12	...	9.8×10^{-7}	0.22
2) PLE with z_{cut} *	1.87	3.03	44.17	2.52	1.39	8.9×10^{-7}	0.31
3) LDDE/a *	0.62^c	2.25^c	44.13	5.40^c	1.55^c	1.4×10^{-6} ^{c,d}	0.11
4) LDDE/b*	0.68	2.05	44.03	4.66	1.55^c	2.0×10^{-6} ^{d}	0.47
5) PLE$^\diamond$	1.93	2.96	44.23	2.19	...	8.6×10^{-7}	0.48
6) PLE with z_{cut} $^\diamond$	1.92	2.96	44.22	2.23	2.31	8.5×10^{-7}	0.73
68% confidence errors	$^{+0.12}_{-0.16}$	$^{+0.11}_{-0.09}$	$^{+0.13}_{-0.15}$	$^{+0.13}_{-0.14}$	$^{+0.56}_{-0.25}$	8%	

(∗) $(\Omega_m, \Omega_\Lambda)$=(1.0,0.0); (⋄) $(\Omega_m, \Omega_\Lambda)$=(0.3,0.7)
(a) Mpc^{-3}(10^{44}erg s^{-1})$^{-1}$; (b) χ^2 probability; (c) fixed; (d) Mpc^{-3}(erg s^{-1})$^{-1}$

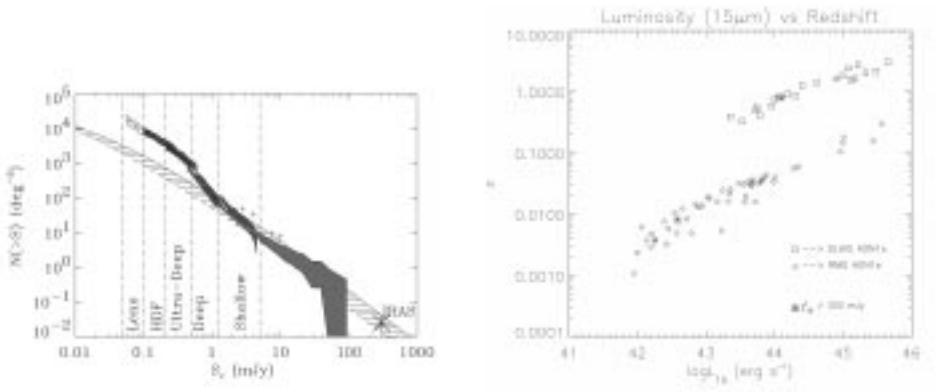

Figure 4. a) Integral Counts at 15μm from the Final Analysis of the ELAIS-S1 Region (light grey shaded area). Also plotted the faintest IRAS surveys and the deep ISOCAM surveys (dark grey shaded areas). b) The luminosity/redshift distribution of our 22 ELAIS-S1 AGN1 and the 55 AGN1 coming from the RMS catalogue.

An initial catalog for S1 (J2000, $\alpha : 00^h34^m44^s$, $\delta : -43^O34'44''$), covering and area of 3.96 deg^2, was produced using the Imperial College data reduction technique ("Preliminary Analysis", Serjeant et al., 2000). Optical identifications were possible thanks to an extensive R-band CCD survey, performed with the ESO/Danish 1.5m telescope. The spectroscopic follow-up program, carried out at the AAT at the AAO and the 3.6m/NTT at ESO/La Silla, of 114 sources in S1 fainter than R$\sim$17.0 provided the sample presented here.

The ELAIS-S1 field has also been completely covered in the radio at 1.4 GHz down to 0.3 mJy (Gruppioni et al., 1999), and 50% covered in the X-rays with BeppoSAX (Alexander et al., 2001). Now the Final Analysis has been completed by the ELAIS team in Bologna. The resulting complete catalog includes more that 450 sources, with fluxes at 15μm down to 0.5 mJy and selected with S/N>5 (Lari et al., 2001).

For many years there has been a gap in flux between the brighter samples (>300 mJy), coming from the IRAS surveys and covering large sky areas, and the deep/pencil-bin surveys carried out by ISO at much fainter fluxes (<1 mJy). In the integral counts derived from the final analysis (Figure 4a, Gruppioni et al., in prep) we see how the ELAIS survey fills the whole flux range between these two regimes.

The nature of the objects identified by the spectroscopic follow-up is:

– High star-forming galaxies (45%);
– AGNs (type 1 & 2) represent 30%;
– 15% of galaxies dominated by absorption lines;
– 4% of late-type stars;
– 6% of unclear classification (AGN2, Starburst, LINER).

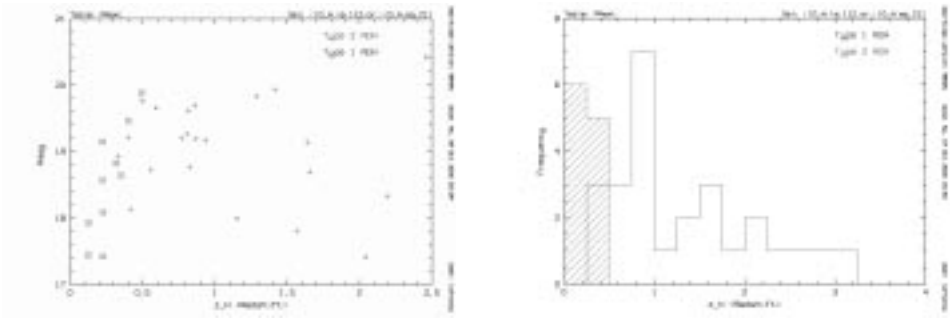

Figure 5. a) Distribution of AGN1 (plus symbols) and AGN2 (crossed squares) in the redshift-Rmag space. While the R-magnitude distribution is constant with a large spread for AGN1, AGN2 show a trend with redshift, becoming fainter than R=20.0 at $z \sim 0.5$. b) Distribution in the redshift space of AGN1 and AGN2 (shaded area). If we consider the redshift bin z=[0.0,0.5] the ratio of AGN2/AGN1 becomes 11/3$\sim$4.

Table 2. The percentages of all objects with emission lines

		AGN1	AGN2	ELG	LINERS
ELAIS-S1	%	20	10	50	2
15μm	<z>	1.4	0.3	0.2	0.3
IRAS	%	6	17	54	23
12μm	<z>	0.04	0.015	0.014	0.007

Note - IRAS subsample from Alexander & Aussel (2000)

The observed ratio of the number of type 2 with respect to type 1+2 AGNs is 1/3. But this result is mainly an artifact due to the different selection functions of the sample for AGN1 and AGN2. The optical selection introduced in the spectroscopic follow-up ($17.0<R<20.0$) seems to be at the origin of the lack of type 2 AGNs beyond $z \sim 0.5$. As a matter of fact, in Figure 5a a trend is observed for AGN2 with optical magnitudes being fainter at larger redshifts. In Figure 5b the redshift distributions of AGN1 and AGN2 are shown. In the redshift bin where type 2 AGNs are observed (z=0.0-0.5), the ratio AGN2/AGN1 becomes $\sim$4, similar to the predictions of the standard unification model. The follow-up campaign to be carried out at September/November 2001 with the ESO telescopes will verify if this trend is seen at fainter and brighter optical fluxes.

3.2. The Evolution of AGN1

We have assumed H_0=75 km/s/Mpc and a (Ω_m,Ω_Λ)=(1.0,0.0) cosmology. Our ELAIS preliminary sample of 22 AGN1 is statistically significant enough to compute a first estimate on the evolution of these objects in the Mid-IR. The mean SED from Elvis et al. (1994) for radio quiet QSOs was adopted as a good representation of our sources. K-corrections were computed for each of the two different filters: ISOCAM-LW3 at 15μm and IRAS 12μm.

A subsample of AGN1 was extracted from the catalog of Rush, Malkan & Spinoglio (1993), as representative in the local universe of this type of ob-

jects. The catalog consists of a sample of galaxies selected at 12μm from the IRAS Point Source Catalog PSCv2, and is complete down to 0.3 Jy. With the computed K-correction, 15μm luminosities (over ISOCAM filter) were derived. Figure 4b represents, in the luminosity-redshift space, all AGN1 coming from ELAIS and RMS that have been used in this analysis.

Similarly to what found in the optical and in the X-rays we adopted a smooth double power-law for the space density distribution of QSOs in the local universe (z=0):

$$\frac{d\Phi(L_{\rm IR}, z=0)}{d{\rm Log}L_{\rm IR}} = {\rm C}\left[({\rm L_{IR}/L_*})^{\alpha} + ({\rm L_{IR}/L_*})^{\beta}\right]^{-1},$$

the standard luminosity evolution (PLE) has been adopted: $L^*_{\rm IR}(z) = L^*_{\rm IR}(0)(1+z)^k$. A parametric, unbinned maximum likelihood method was used to fit the evolution and luminosity function parameters simultaneously (Marshall et al., 1983) at 15μm. Since ELAIS identifications were not only flux limited at 15μm, but also in their R-band magnitude ($17.0 < {\rm R} < 20.0$), a factor $\mathbf{\Theta}$ was introduced in the function 'S' to be minimized

$${\rm S} = -2\sum_{\rm i=1}^{\rm N}\ln[\Phi({\rm z_i, L_i})] + \iint \Phi({\rm z,L})\Omega({\rm z,L})\,\mathbf{\Theta}\,\frac{\rm dV}{\rm dz}{\rm dzdL},$$

to correct for incompleteness, and only applied to the ELAIS sample. This factor $\mathbf{\Theta}$ represents the probability that a source with a given luminosity at 15μm ($\rm L_{15}$) has a R-magnitude ($\rm L_R$) between the limits of the sample (17.0<R<20.0),

$$\mathbf{\Theta}({\rm z,L})\,(17.2 < {\rm R} < 20.0 \mid {\rm L_{15}})\,.$$

and was derived taking into account the internal spread in the SED.

From the total available list of AGN1 of the sample, the number of objects that entered the computation was defined as:

- RMS: sources with $\rm F_{12\mu m} > 300$ mJy, 42 sources
- ELAIS: sources with $\rm F_{15\mu m} > 1$ mJy, and $17.0 < {\rm R} < 20.0$, 21 sources

The resulting estimate of the LF of AGN1 at 15μm with its parameters is shown in Figure 6. The probability that our data have been drawn from the fitted PLE model is 0.15, as given by the 2DKS test. The PLE model adopted here could not be sufficient to represent the space density of our sources, some density evolution may be required. Currently we are studying different parameterizations taking into account some degree of density evolution.

For the derived PLE model the contribution of AGN1 to the CIRB at 15μm is $I = 2.86\cdot10^{-10}$ Wm^{-2}sr^{-1} which corresponds $\sim 7\%$ of the total CIRB in this band if we take a value for the total intensity of the background of $I = 4.0\cdot10^{-9}$ Wm^{-2}sr^{-1} (Hauser & Dwek 2001; Hauser 2001). At maximum, the total contribution of AGNs to the background at 15μm can be as high as $I = 1.4\cdot10^{-9}$ Wm^{-2}sr^{-1} (35%), under the extreme assumptions: 1) that AGN2 are as much bright as AGN1 at 15 μm, 2) that the ratio of type 2 to type 1 AGN is 4 at all redshifts, and 2) that AGN2s evolved with the same LF of AGN1.

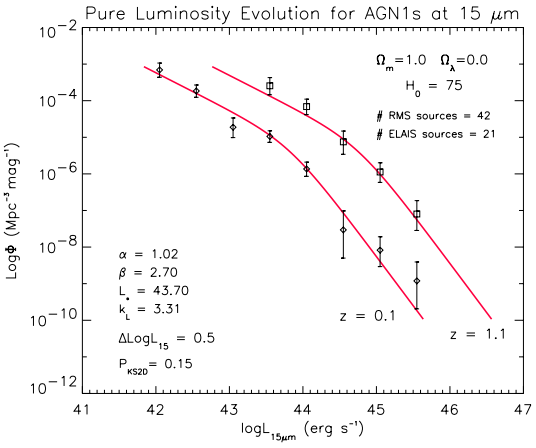

Figure 6. PLE fit to our 63 total sources (RMS + ELAIS-S1). The densities have been corrected for evolution within the redshift bins.

3.3. Conclusions

Thanks to the spectroscopic campaigns carried out on the HELLAS and ELAIS catalogues, we have been able to build up statistical significant samples of AGN1 and estimate the evolution of their LF in the hard X-rays and IR.

In the hard X-rays we have been able to double the number of hard X-ray AGN1 available for statistical analysis at fluxes in the range $f_{2-10keV} \sim 10^{-12} - 10^{-13.5} erg\ cm^{-2} s^{-1}$. In total we have used 74 AGN1 at these fluxes, which combined with the local sample of Grossan (1992) have allowed to show directly the shape of the LF of AGN1 as function of redshift. In the IR, our sample of 22 AGN1 has allowed the first estimate of the evolution of the LF at 15μm.

Both LFs are fairly well represented by a double-power-law-function with a significant cosmological evolution according to a PLE model with $L(z) \propto (1+z)^k$. However, there are some evidences of density evolution (LDDE) at faint luminosities.

Acknowledgments. Based on observations collected at the European Southern Observatory, Chile, ESO N°: 62.P-0783, 63.O-0117(A), 64.O-0595(A), 65.O-0541(A). We thank the BeppoSAX SDC, SOC and OCC teams for the successful operation of the satellite and preliminary data reduction and screening. This research has made use of the NASA/IPAC Extragalactic Database (NED) which is operated by the Jet Propulsion Laboratory, California Institute of Technology, under contract with the National Aeronautics and Space Administration. This research has been partially supported by ASI contracts ARS-99-75, ASI 00/IR/103/AS, ASI I/R/107/00, MURST grants Cofin-98-02-32, Cofin-99-034, Cofin-00-02-36, Chandra X-ray center grant G01-2100X, and a 1999 CNAA grant.

References

Akiyama, M., Ohta, K., Tamura, N., et. al., 2000, ApJ, 532, 700

Alexander, D., Aussel H. 2000, in the Springer Lecture Notes of Physics Series, ISO Surveys of a Dusty Universe, astro-ph/0002200

Alexander, D., La Franca, F., Fiore, F. et al. 2001, ApJ, 554, 18

Barger, A.J., Cowie, L.L., Mushotzky, R.F., Richards, E.A. 2001, AJ, 121, 662

Boyle, B.J., Georgantopoulos, I., Blair, A.J., Stewart G.C., Griffiths, R.E., Shanks, T., Gunn, K.F., Almaini. O. 1998, MNRAS, 296, 1

Boyle, B.J, Shanks T., Croom, S.M., Smith R.J., Miller L., Loaring N., Heymans C. 2000, MNRAS, 317, 1014

Brandt, W.N., Alexander, D.M., Hornschemeier, A.E., et al., 2001., AJ, in press, astro-ph/0108404

Ceballos, M.T., Barcons, X. 1996, MNRAS, 282, 493

Chen L.W., Fabian A.C., Gendreau K.C. 1997, MNRAS,285, 449

Comastri A., Fiore F., Vignali C., Matt G., Perola G.C., La Franca F. 2001, MNRAS, in press, astro-ph/0105525

Della Ceca, R., Maccacaro T., Gioia I., Wolter A., Stocke J.T. 1992, ApJ, 389, 491

Elvis, M., Wilkes, B.J. et al. 1994, ApJS, 95, 1

Fiore, F., La Franca, F., Giommi, P., et al. 1999, MNRAS, 306, L55

Fiore, F., La Franca, F., Vignali, C., Comastri, A., Matt, G., Perola G.C., Cappi, M., Elvis M., Nicastro, F. 2000, New Astronomy, 5, 143

Fiore, F., Giommi, P., Vignali, C., et al. 2001, MNRAS, in press, astro-ph/0105524

Grossan, B.A. 1992, PhD thesis, MIT

Gruppioni, C. et al. 1999, MNRAS, 304, 199

Hauser, M. G. 2001, in Proc. IAU Symposium 204, The Extragalactic Infrared Background and its Cosmological Implications, Astron. Soc. Pac. Conf. Ser., vol. 204, p. 101, astro-ph/0105550

Hauser, M. G., Dwek, E. 2001, Annual Reviews of Astronomy and Astrophysics, 2001, Vol. 39, in press, astro-ph/0105539

La Franca F., Cristiani S. 1997, AJ, 113, 1517

Lari, C., Pozzi, F., Gruppioni, C. et al. 2001, MNRAS , 325, 1173

Marshall, H.L., Avni, Y., Tananbaum, H., Zamorani, G. 1983, ApJ, 269, 35

Miyaji T., Hasinger G., Schmidt M. 2000, A&A, 353, 25

Pompilio, F., La Franca, F., Matt, G. 2000, A&A, 353, 440

Rush, B., Malkan, M.A., Spinoglio, L. 1993, ApJS, 89, 1 (RMS)

Serjeant, S. et al. 2000, MNRAS, 316, 768

Vignali C., Comastri A., Fiore F., La Franca F. 2001, A&A, 370, 900